

# Effect of Si Co Doping on Ferromagnetic Properties of GaGdN

J.K. HITE,<sup>1</sup> R.M. FRAZIER,<sup>1</sup> R.P. DAVIES,<sup>1</sup> G.T. THALER,<sup>1</sup>  
C.R. ABERNATHY,<sup>1</sup> S.J. PEARTON,<sup>1,4</sup> J.M. ZAVADA,<sup>2</sup> E. BROWN,<sup>3</sup>  
and U. HÖMMERICH<sup>3</sup>

1.—Department of Materials Science and Engineering, University of Florida, Gainesville, FL 32611, USA. 2.—U.S. Army Research Office, Research Triangle Park, Florida, NC 27709, USA. 3.—Department of Physics, Hampton University, Hampton, VA 23668, USA. 4.—E-mail: spear@mse.ufl.edu

Single-phase GaGdN and GaGdN:Si films were grown on sapphire substrates by gas source molecular beam epitaxy using solid Gd, Ga, and Si sources and active nitrogen derived from a RF nitrogen plasma source. The undoped films were highly resistive films but became conductive with the addition of Si. Superconducting quantum interference device magnetometry indicated room-temperature ferromagnetism in both types of materials. Structural defects had a strong influence on the magnetic ordering of the material, as seen in a drastic reduction of magnetic moment with degrading crystalline quality. Magnetization of the codoped film increased with Si content, reaching levels higher than that of the undoped material. The Gd-doped AlN films grown in a similar fashion also displayed Curie temperatures above room temperature.

**Key words:** GaN, spintronics, AlN

## INTRODUCTION

The field of spin-based electronics, or spintronics, has emerged as a candidate in the search for the next technological breakthrough in both electronics and photonics. By controlling the quantum spin state of electrons, this field has potential for increased speed, power efficiency, and storage density in devices.<sup>1–4</sup> One approach in which to achieve this is with dilute magnetic semiconductors (DMSs). Recent interest has focused on GaN as a base for DMSs due to its wide band gap, robust nature, and well-established manufacturing base for light-emitting diodes and laser diodes. Transition metal dopants in GaN have been extensively studied,<sup>5–20</sup> but the rare earth elements have lately gained momentum as a dopant for dilute magnetic semiconductor applications.<sup>21–23</sup> There is potential for incorporating this type of material into applications such as spin valves, magnetic tunnel junctions, and spin LEDs. The ability to manipulate the Fermi level of the material would make it an even better

candidate for device integration than the transition metal doped GaN, where typically 3–10 at.% of the element must be incorporated, disrupting the normal electrical and photonic properties. By sharp contrast, concentrations of Gd in the  $10^{15}$ – $10^{18}$  cm<sup>-3</sup> range have proven effective in producing room-temperature ferromagnetism in GaN.<sup>21–23</sup> These reports of colossal magnetic moments with Curie temperatures above 400 K in Gd-doped GaN (GaN:Gd) thin films have sparked interest in exploring other rare earth–nitride systems as candidate materials for spintronic devices. The doping of nitrides with rare earth ions may serve as an alternative to transition metal doping with the possibility of room-temperature ferromagnetism mediated either by carriers or by conduction through bands induced by the rare earth ions. In addition, because the rare earth dopants may be optically active in these materials, magnetic and optical functionality on a single chip may be possible.

This paper reports on the magnetic properties of GaGdN grown by rf plasma-assisted molecular beam epitaxy, including the effects of incorporation of extra shallow donors by codoping GaN with both Gd and Si.

(Received July 21, 2006; accepted October 27, 2006;  
published online December 28, 2006)

## EXPERIMENTAL

GaGdN and GaGdN:Si were grown by gas source molecular beam epitaxy (MBE) using solid Gd, Ga, and Si sources heated in effusion cells and nitrogen from an Oxford rf plasma head. A Veeco P75 metal organic chemical vapor deposition chamber produced the 2- $\mu\text{m}$  GaN on *c*-plane sapphire buffer layers used as substrates for the MBE films. Using this starting material eliminates the need for steps such as nitridation and nucleation needed to bridge the lattice gap when starting on sapphire. It also improves the quality of the epitaxial film as compared to those grown on low-temperature MBE buffers.<sup>7,24</sup> The native oxide was removed prior to MBE growth using an etch progressing through HCl, UV ozone exposure, buffered oxide etch, and a DI water rinse. The epitaxial films were grown using a thermocouple measured substrate temperature of 700°C with a nitrogen flow rate of 1.6 sccm. The Ga cell was held constant throughout the growth runs at 785°C, while the Gd cell was varied from 900°C to 1,125°C. Reflection high energy electron diffraction (RHEED) was used to monitor films during growth. When codoping, the Si cell temperature ranged from 1,000°C to 1,200°C. The codoped material was grown to a film thickness of 0.15  $\mu\text{m}$ , while the GaGdN was grown to varying thicknesses. A few runs were also made of Gd-doped AlN, with the Gd cell temperature varied from 1,000°C to 1,150°C. In some cases, Gd was implanted into *p*-type GaN films on sapphire, both as a calibration for secondary ion mass spectrometry (SIMS) measurements and for measuring the magnetic properties.<sup>22</sup> These films were annealed at 700–1,000°C prior to the magnetic measurements.

## RESULTS AND DISCUSSION

The singly doped films showed an optimal RHEED pattern with  $1 \times 3$  reconstruction at 0.1  $\mu\text{m}$ , which is shown in Fig. 1. After about 0.12  $\mu\text{m}$ , this two-dimensional (2-D) growth pattern degenerated into one indicative of 2-D/three-dimensional (3-D) growth and continued to degrade to a 3-D growth pattern with increasing thickness. After becoming 2-D/3-D, the reconstruction pattern disappeared. The codoped material exhibited 2-D growth and  $1 \times 3$  reconstruction through a thickness of 0.15  $\mu\text{m}$ . The growth rate for all the films was  $\sim 0.1 \mu\text{m/h}$ . The addition of Si doping helped smooth out the surface, as the codoped material grew in the 2-D mode for thicker films. Comparisons between the two materials were restricted to those with similar crystalline structure as determined by RHEED and x-ray diffraction. The Gd flux did not change the RHEED pattern and there was no evidence of Gd acting as a surfactant. Atomic force microscopy (AFM) scans shown at the bottom of Fig. 1 determined the root mean surface roughness of both films to be approximately 1.8 nm.

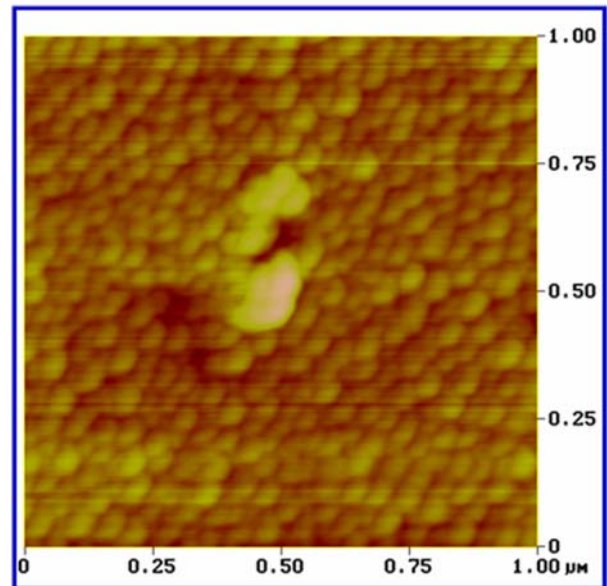
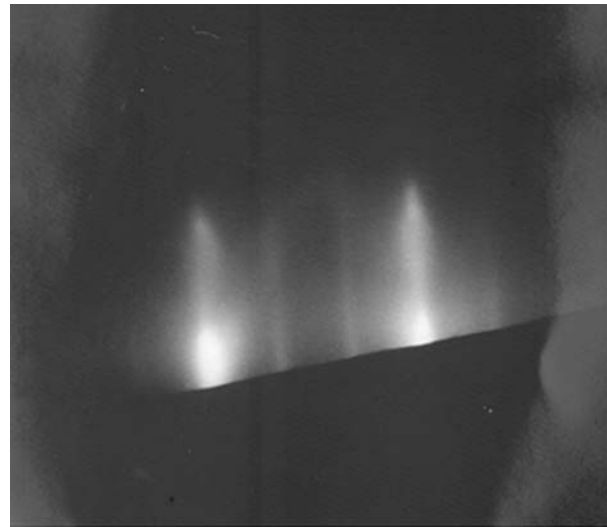


Fig. 1. RHEED pattern of 2-D growth for GaGdN:Si (top) and AFM scan of 0.15- $\mu\text{m}$ -thick GaGdN (bottom).

Compositional analysis of the films was carried out using both x-ray diffraction (XRD) in a Philips powder diffractometer and SIMS using  $\text{Cs}^+$  and  $\text{O}_2^+$  ions performed by Evans Analytical Group. No second phases were observed via XRD, with the only peaks originating from GaN and sapphire. With the extremely low Gd flux used during growth, this is not unexpected. Additional examination via transmission electron microscopy (TEM) showed orderly lattice matching between the buffer and films (Fig. 2) without any evidence of clustering. In further investigation by SIMS, the concentration of Gd was under the detection level of  $\sim 2 \times 10^{17}$  atoms/ $\text{cm}^3$ . The films of Dhar et al.<sup>17,21</sup> were grown with higher Gd concentrations, up to  $2 \times 10^{19}$   $\text{cm}^{-3}$ , and they were also able to grow films up to 700-nm thick without loss of crystal quality. This suggests that use of  $\text{NH}_3$  rather than rf-plasma activated  $\text{N}_2$

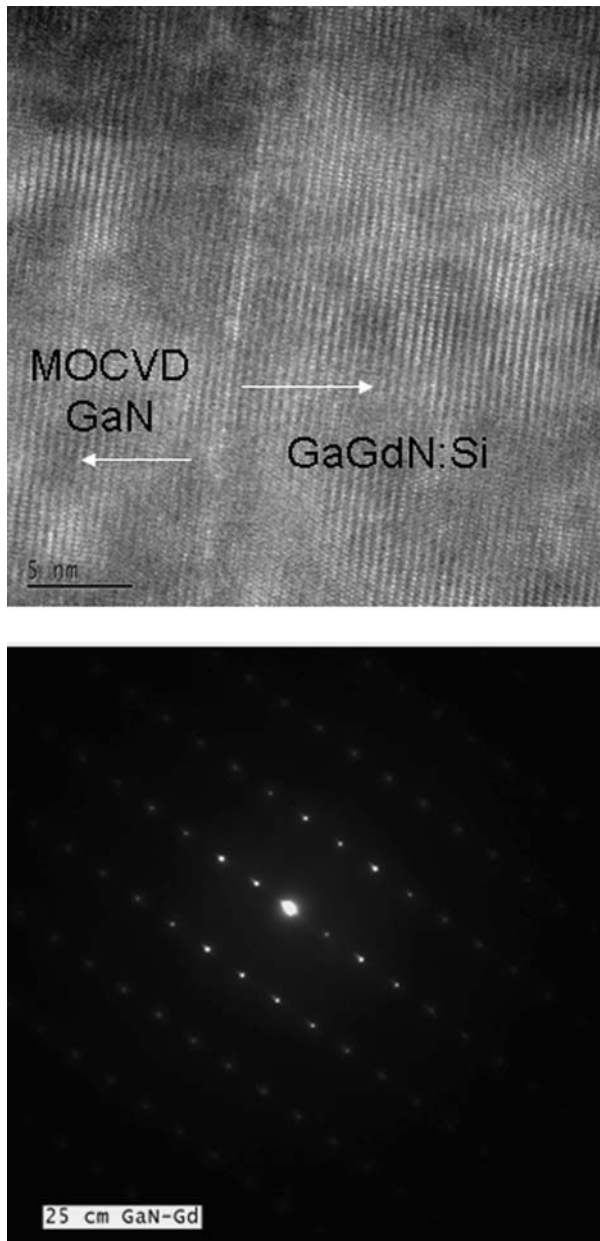


Fig. 2. TEM images of GaGdN:Si showing lattice structure (top) and diffraction pattern (bottom).

provides a higher surface mobility of the ad-atoms. The Gd is a large atom (atomic radius  $\sim 2.5 \text{ \AA}$ ) relative to both Ga ( $\sim 1.8 \text{ \AA}$ ) and N ( $\sim 0.75 \text{ \AA}$ ), and it might be expected that it is difficult to incorporate on substitutional sites if the growth temperature or Ga flux is too high. The use of  $\text{NH}_3$  as the nitrogen precursor appears to expand the range of growth conditions that allow higher concentrations of Gd to be incorporated. Photoluminescence of the films with a Nd:YAG excitation source showed weak band edge peaks from the GaN at 364 nm, which were stronger than the comparable Gd-implanted films, as shown in Fig. 3. This suggests that the incorpo-

ration of Gd during growth is preferable for maintaining the optical properties of the GaN.

Magnetic characterization of the films was carried out in a quantum design superconducting quantum interference device magnetometer. All measurements were taken with the applied field parallel to the sample surface. The diamagnetic contribution from the substrate and sample holder was subtracted out, and the results were normalized to volume. Measurements of magnetization versus temperature were done in an applied field of 200 Oe, and magnetization versus applied field measurements were taken at 10 K and 300 K. Both Si codoped and Gd only-doped samples showed ferromagnetism up to room temperature. Examples for the Gd-only samples are shown in Fig. 4 as a function of Gd cell temperature. No magnetization was observed for the lowest ( $900^\circ\text{C}$ ) or highest ( $1,125^\circ\text{C}$ ) Gd cell temperatures. We emphasize that only the Gd cell temperature was varied in these experiments. This may be a result of insufficient Gd concentration at the lowest temperatures and nonsubstitutional incorporation at the highest temperature, but we have no direct evidence of this speculation. The saturation magnetization was highest at an intermediate cell temperature of  $1,050^\circ\text{C}$  in the case of these singly doped samples. We have seen similarly sharply peaked curves for the optimal magnetization with other magnetic dopants in GaN, indicating the sensitivity of magnetization to magnetic ion concentration and solubility. Figure 5 shows hysteresis plots at different temperatures from GaGdN grown with a Gd cell temperature of  $1,050^\circ\text{C}$ . There was little decrease in saturation magnetization, suggesting a Curie temperature above 350 K, a fact confirmed by field-cooled/zero field-cooled magnetization measurements.

Similar basic trends were seen with the Si-codoped samples. A representative hysteresis curve for the Si codoped samples is shown in Fig. 6 along with the zero field-cooled/field-cooled traces. The saturation magnetization increased linearly with Si cell temperature, as shown in Fig. 7. The GaGdN film exhibited the highest saturation magnetization when grown with a 2-D RHEED pattern. This dependence of magnetization on crystalline quality has been seen in other materials.<sup>7,24</sup> At the highest end of  $T_{\text{Si}}$ , the GaGdN:Si showed higher magnetization than the GaGdN.

Hall measurements performed at room temperature provided electrical data on the material. As-grown GaGdN films were highly resistive, but became increasingly conductive with Si incorporation. This is illustrated in Fig. 8. In coordination with the conductivity, carrier concentration and mobility also increased with Si doping. There is also a need to establish the effect of the Si doping on the thermal stability of the GaGdN, because this is important for device applications. Somewhat surprisingly, Dhar et al.<sup>25</sup> also found that Gd-focused ion beam implanted GaN showed room-temperature ferromagnetism and colossal magnetic moment

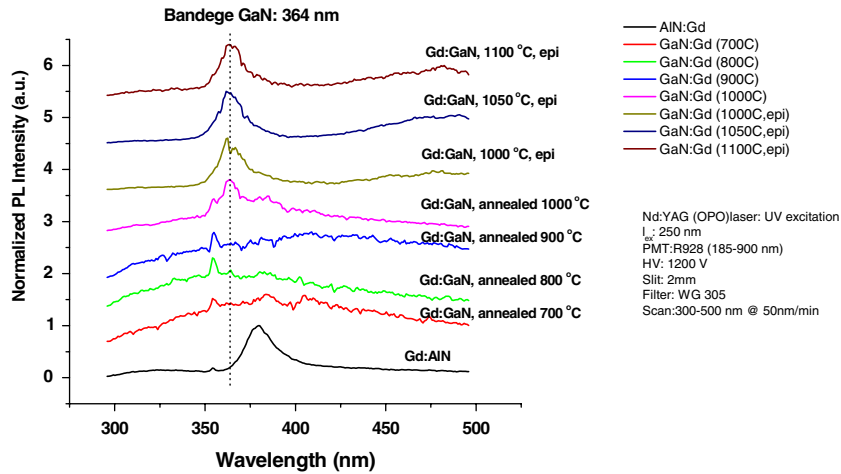


Fig. 3. PL spectra at 4 K of GaN and AlN films doped with Gd during growth or by ion implantation and subsequent annealing.

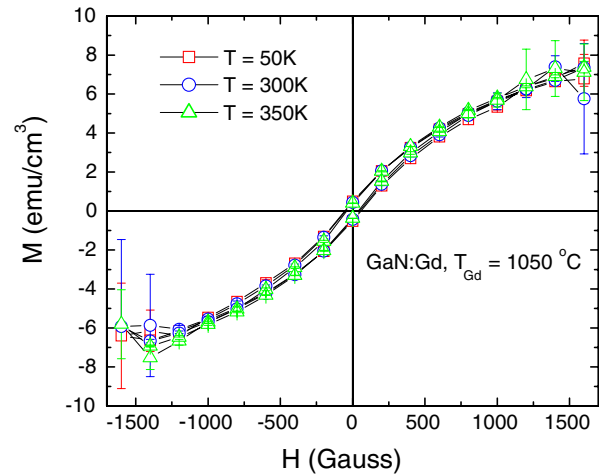
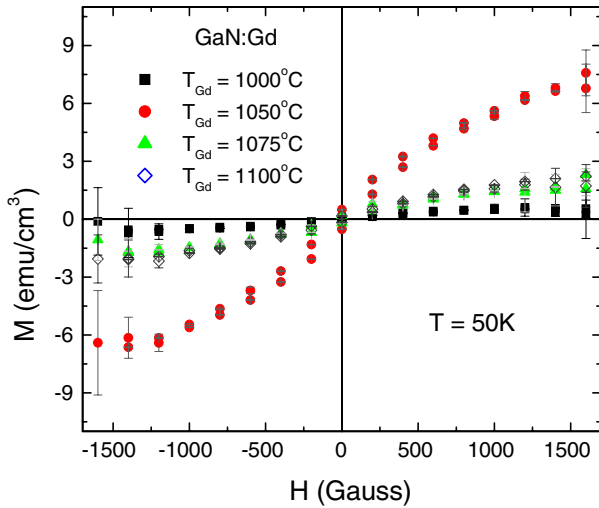


Fig. 5. Hysteresis plots at different temperatures from GaGdN grown with a Gd cell temperature of 1,050°C.

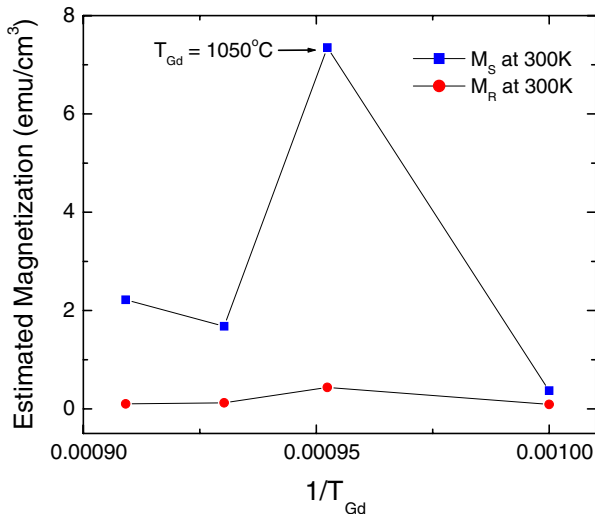


Fig. 4. Magnetization versus field curves for Gd-doped GaN grown with different cell temperatures (top) and saturation and remnant magnetization as a function of inverse Ga cell temperature (bottom).

without any annealing, suggesting that defects play an important role. No thermal stability was reported in that work.

The AlGdN samples also showed room-temperature hysteresis when doped with Gd at a high enough Gd cell temperature. Figure 9 shows hysteresis loops at room temperature from AlGdN doped with Gd at different Gd cell temperatures (top) and field-cooled/zero field-cooled magnetization (bottom). The optimum cell temperature was 1,075°C and the magnetization is larger in these samples than in AlMnN and AlCrN reported previously and grown under similar conditions.<sup>26-29</sup>

### CONCLUSIONS

In conclusion, evidence is found that the RT ferromagnetism of GaGdN has been retained and may be improved by the addition of Si. The magnetic behavior is influenced by the degree of Si incorporation. In addition, the insulating GaGdN is

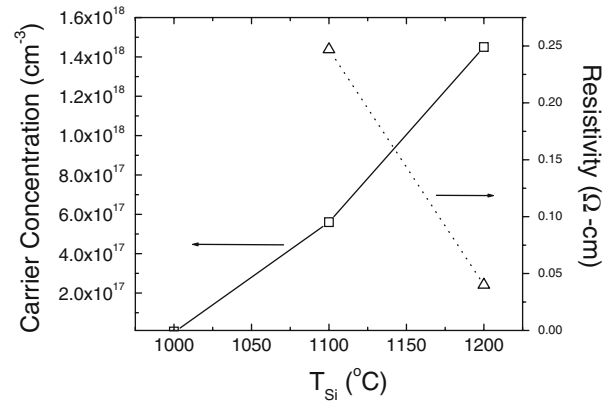
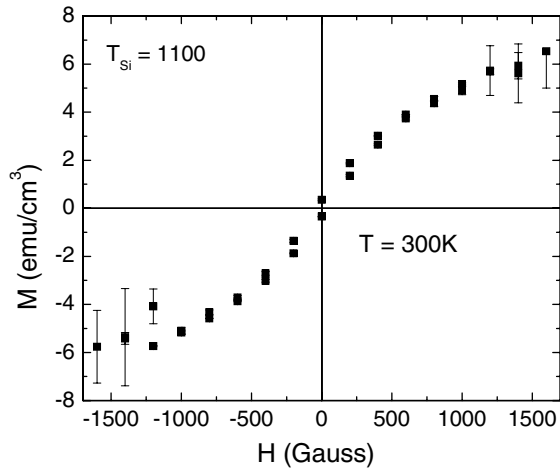


Fig. 8. Carrier concentration and resistivity of GaGdN versus Si cell temperature.

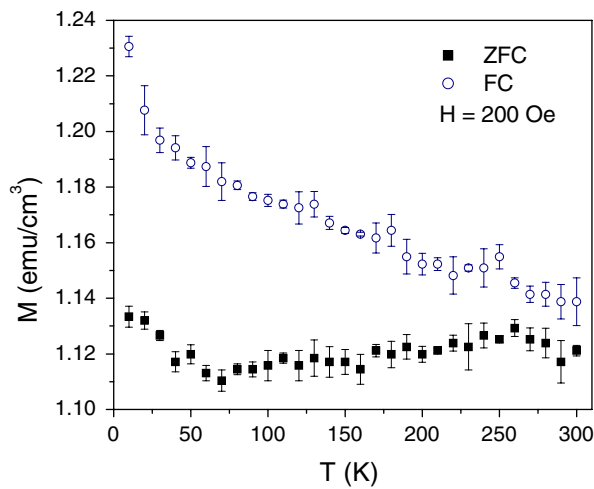


Fig. 6. Magnetization versus applied field for GaGdN:Si samples grown at a Si cell temperature of  $T_{Si} = 1,100^{\circ}C$  (top) and field-cooled/zero field-cooled magnetization (bottom). The Gd cell temperature was  $1,050^{\circ}C$ .

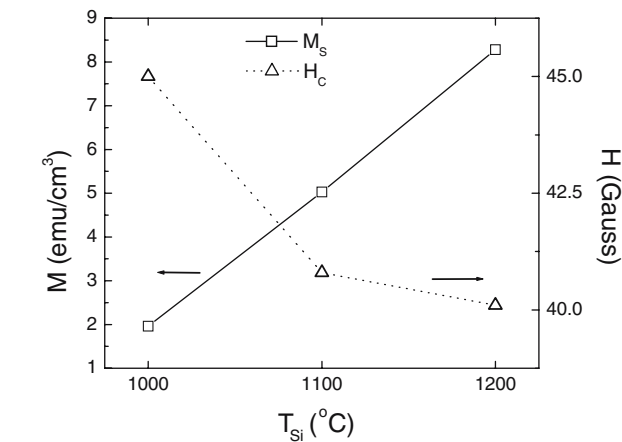
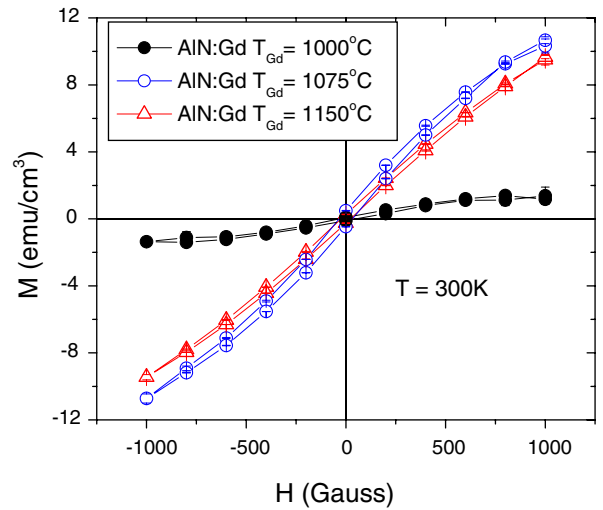


Fig. 9. Hysteresis loops at room temperature from AlGdN doped with Gd at different Gd cell temperatures (top) and field-cooled/zero field-cooled magnetization (bottom).

Fig. 7. Saturation magnetization and coercivity versus Si cell temperature for GaGdN:Si. The Gd cell temperature was  $1,050^{\circ}C$ .

transformed into conductive  $n$ -type material with the addition of Si. The ability to control the conductivity while retaining room-temperature ferromagnetism makes GaGdN:Si a promising candidate for developing devices out of dilute magnetic semiconductors.

### ACKNOWLEDGEMENTS

The work at the University of Florida was supported by the Army Research Office under Contract No. W911-NF-0410296. The help of Kerry Seibin, UF MAIC facility, with the TEM analysis is appreciated.

### REFERENCES

1. S. von Molnar, *J. Superconductivity: Incorporating Novel Magnetism* 16, 1 (2003).
2. S.A. Wolf, D.D. Awschalom, R.A. Buhrman, J.M. Daughton, S. von Molnar, M.L. Roukes, A.Y. Chtchelkanova, and D.M. Treger, *Science* 294, 1488 (2001).
3. S. Von Molnar and D. Read, *J. Magn. Mag. Mater* 242–245, 13 (2002).
4. S.J. Pearnton, et al., *J. Appl. Phys.* 93, 1 (2003).
5. M.L. Reed, N.A. El-Masry, H.H. Stadelmaier, M.E. Ritums, N.J. Reed, C.A. Parker, J.C. Roberts, and S.M. Bedair, *Appl. Phys. Lett.* 79, 3473 (2001).
6. G.T. Thaler, et al., *Appl. Phys. Lett.* 80, 3964 (2002).
7. G.T. Thaler, R.M. Frazier, C.R. Abernathy, and S.J. Pearnton, *Appl. Phys. Lett.* 86, 131901 (2005).
8. H. Asahi, Y.K. Zhou, M. Hashimoto, M.S. Kim, X.J. Li, S. Emura, and S. Hasegawa, *J. Phys.: Condens. Matter* 16, S5555 (2004).
9. N. Teraguchi, A. Suzuki, Y. Nanishi, Y.-K. Zhou, M. Hashimoto, and H. Asahi, *Solid State Commun.* 122, 651 (2002).
10. I. Zutic, J. Fabian, and S.D. Sarma, *Rev. Mod. Phys.* 76, 323 (2004).
11. T. Dietl, H. Ohno, F. Matsukura, J. Cibert, and D. Ferrand, *Science* 287, 1019 (2000).
12. K.H. Kim, K.J. Lee, D.J. Kim, H.J. Kim, Y.E. Ihm, D. Djayaprawira, M. Takahashi, C.S. Kim, C.G. Kim, and S.H. You, *Appl. Phys. Lett.* 82, 1775 (2003).
13. Y.L. So, G. Kiioseoglou, S. Kim, S. Huang, Y.H. Koo, S. Kuwarbara, S. Owa, T. Kondo, and H. Munekata, *Appl. Phys. Lett.* 79, 3926 (2001).
14. S. Kuwabara, T. Kondo, T. Chikyuu, P. Ahmet, H. Munekata, *Jpn. J. Appl. Phys.* 40, L724 (2001).
15. G.T. Thaler, et al., *Appl. Phys. Lett.* 80, 4357 (2002).
16. H. Hori, S. Sonoda, T. Sasaki, Y. Yamamoto, S. Shimizu, K. Suga, and K. Kindo, *Physica B* 324, 142 (2002).
17. S. Dhar, O. Brandt, A. Trampert, L. Daweritz, K.J. Friedland, K.H. Ploog, J. Keller, B. Beschoten, and G. Guntherhold, *Appl. Phys. Lett.* 82, 2077 (2003).
18. M.C. Park, K.S. Huh, J.M. Hyong, J.M. Lee, J.Y. Chung, K.I. Lee, S.H. Han, and W.Y. Lee, *Solid-State Commun* 124, 11 (2002).
19. I.A. Buyanova, et al., *J. Electron. Mater* 33, 467 (2004).
20. I.A. Buyanova, et al., *Appl. Phys. Lett.* 84, 2599 (2004).
21. S. Dhar, O. Brandt, M. Ramsteiner, V.F. Sapega, and K.H. Ploog, *Phys. Rev. Lett.* 94, 037205 (2005).
22. S.Y. Han, et al., *Appl. Phys. Lett.* 88, 042102 (2006).
23. G. M. Dalpian, and S.-H. Wei, *Phys. Rev. B* 72, 115201 (2005).
24. G.T. Thaler, R.M. Frazier, B.P. Gila, J. Stapleton, M. Davidson, C.R. Abernathy, S.J. Pearnton, and C. Segre, *Appl. Phys. Lett.* 84, 2578 (2004).
25. S. Dhar, T. Kammermeier, A. Ney, L. Perez, K. Ploog, A. Melnikov, and A.D. Wieck, *Appl. Phys. Lett.* 89, 062503 (2006).
26. S.J. Pearnton, D.P. Norton, R. Frazier, S.Y. Han, C.R. Abernathy, and J.M. Zavada, *IEE Proc.-Circuits, Devices Systems* 152, 312 (2005).
27. R. Frazier, G.T. Thaler, J.Y. Liefer, J.K. Hite, B.P. Gila, C.R. Abernathy, and S.J. Pearnton, *Appl. Phys. Lett.* 86, 052101 (2005).
28. A.Y. Polyakov, N.B. Smirnov, A.V. Govorkov, R.M. Frazier, J.Y. Liefer, G.T. Thaler, C.R. Abernathy, S.J. Pearnton, and J.M. Zavada, *J. Vac. Sci. Technol* 22, 2758 (2004).
29. A.Y. Polyakov, N.B. Smirnov, A.V. Govorkov, R.M. Frazier, J.Y. Liefer, G.T. Thaler, C.R. Abernathy, S.J. Pearnton, and J.M. Zavada, *Appl. Phys. Lett.* 85, 4067 (2004).